Optimal Transmission Condition of Nonlinear Optical Pulses in Single-Mode Fibers

Min-Chuan Lin and Sien Chi

Abstract—**Optimal transmission conditions of nonlinear optical pulses in single-mode fibers are presented. When an optical pulse propagates in a fiber, it suffers the fiber loss, group velocity dispersion, and self-phase modulation. An optimal output pulse can be obtained by choosing a suitable optical carrier wavelength and an initial input pulse. The system at the optimal condition not only has more stable performance than the dispersion-free system, but also achieves maximum transmission bitrate for a fixed transmission distance. The bit-length product up to 8550 Gb/s·km or more can be achieved by using dispersion-shifted fibers without amplification.**

Index Terms—**Self-Phase Modulation**

I. Introduction

THE linear optical fiber transmission system has the maximum transmission bitrate when the optical carrier wavelength (λ) coincides with the zero-dispersion wavelength (λ_0), and the bitrate is limited by the second-order dispersion [1]. But the self-phase modulation (SPM) due to index nonlinearity can not be ignored when designing the ultra-high bitrate system operating at $\lambda = \lambda_z$ over a long distance [2]. The interaction among the SPM, fiber loss and group velocity dispersion (GVD), becomes the fundamental nonlinear limitation for ultra-high speed fiber-optic transmission systems [3]. A good strategy to use the index nonlinearity is to adopt the concept of soliton transmission [4] where the SPM cancels the anomalous dispersion when $\lambda > \lambda_0$. Optical solitons have been suggested as possible information carriers in a single-mode fiber resulting in a hundred-fold increase in bandwidth over the dispersion-free system design [5], [6]. The bitrate of a nonlinear transmission system is limited by the GVD, SPM and fiber loss [5], [7], [8]. When decreasing λ close to λ_0, the equivalent soliton order becomes larger for a fixed input power, and the pulse with multi-peaks feature tends to split into subpulses under the influence of the fiber loss [9]. Therefore, the effective pulse widths become broader. If the SPM-broadened optical spectrum spans both sides of λ_0, the components in the normal dispersion region will disperse away due to the interaction between GVD and SPM [9], [10]. On the other hand, when increasing λ away from λ_0, the first-order GVD will dominate and lead to pulse broadening. For a fixed transmission distance, there should exist an optimum input pulse width and a specific carrier wavelength in the anomalous dispersion region to achieve the minimum output pulse width which implies the best received signal quality and the maximum transmission bitrate. In this paper, we will investigate the optimal transmission condition of the nonlinear optical pulses in a fiber without optical amplification.

Manuscript received October 29, 1991; revised May 26, 1992. This work was supported in part by the National Science Council and Telecommunication Laboratories of R.O.C. under contract NSC 80-0417-E009-13.

The authors are with the Institute of Electro-Optical Engineering and Center for Telecommunications Research, National Chiao Tung University, Hsinchu, Taiwan, Republic of China.

IEEE Log Number 9204441.

II. Simulation Model

The electric field in weakly guiding single-mode fiber is separated into a rapidly varying part and an envelope Q via the equation

$$E(x,y,z,t) = \mathrm{Re}\{Q(z,t)R(x,y)\exp[i(\beta_c z - \omega_c t)]\}. \quad (1)$$

Where ω_c indicates the central angular frequency of the light wave and β_c is the wavenumber in the z direction at this frequency; $R(x,y)$ is a linear eigenfunction of the mode excited in the fiber. Here, we define a normalized electric field envelope $q(z,t)$ as

$$q(z,t) = Q(z,t)\sqrt{\int_{-\infty}^{\infty}\int_{-\infty}^{\infty} R^2(x,y)dxdy} \quad (2)$$

then the wave equation obeyed by optical pulses propagating along the single-mode fiber can be reduced to the following nonlinear partial differential equation [11]:

$$i\frac{\partial q}{\partial z} + i\beta_1\frac{\partial q}{\partial t} - \frac{1}{2}\beta_2\frac{\partial^2 q}{\partial t^2} + \gamma|q|^2 q = -i\frac{\alpha}{2}q + i\frac{1}{6}\beta_3\frac{\partial^3 q}{\partial t^3} \quad (3)$$

where β_1, β_2, and β_3 are the first, second and third derivatives of wavenumber β with respect to the angular frequency and evaluated at $\omega = \omega_c$; α is the intensity attenuation coefficient of the guided mode in the fiber and assumed to be 0.2 and 0.35 dB/km for 1.55- and 1.3-μm windows, respectively; γ is the nonlinearity coefficient defined by

$$\gamma = \frac{2\pi n_2}{\lambda A_{\mathrm{eff}}} \quad (4)$$

where λ is the optical carrier wavelength, n_2 is the nonlinear-index coefficient and $n_2 = 3.2 \times 10^{-16}$ cm^2/W for SiO_2 [11]; the parameter A_{eff} is known as the effective core area given by

$$A_{\mathrm{eff}} = \frac{\left(\int_{-\infty}^{\infty}\int_{-\infty}^{\infty}|R(x,y)|^2 dx\,dy\right)^2}{\int_{-\infty}^{\infty}\int_{-\infty}^{\infty}|R(x,y)|^4 dx\,dy}. \quad (5)$$

Here, A_{eff}'s are assumed to be 25 and 50 μm^2 for the fibers in 1.55- and 1.3-μm windows, respectively. If we make the following transformations:

$$\tau = (t - \beta_1 z)/T_0 \tag{6}$$

$$\xi = z|\beta_2|/T_0^2 \tag{7}$$

$$u = qT_0\sqrt{(\gamma/|\beta_2|)} \tag{8}$$

where T_0 is an arbitrary time scale, (3) will be reduced to the modified nonlinear Schroedinger equation [11]

$$i\frac{\partial u}{\partial \xi} + \frac{1}{2}\frac{\partial^2 u}{\partial \tau^2} + |u|^2 u = i\delta\frac{\partial^3 u}{\partial \tau^3} + i\Gamma u \tag{9}$$

where $\Gamma = \alpha T_0^2/2|\beta_2|$ is the normalized electric field attenuation coefficient and $\delta = \beta_3/6T_0|\beta_2|$ is the normalized second-order dispersion coefficient. The input optical power required for $|u(\xi = 0, \tau = 0)|^2 = 1$ is

$$P_0 = \frac{|\beta_2|}{\gamma T_0^2}. \tag{10}$$

The dispersion curve used to calculate β_2 and β_3 is approximated by the 3-term Sellmeier equation [12]

$$n^2 - 1 = \frac{B_1\lambda_1^2}{\lambda^2 - \lambda_1^2} + \frac{B_2\lambda_2^2}{\lambda^2 - \lambda_2^2} + \frac{B_3\lambda_3^2}{\lambda^2 - \lambda_3^2} \tag{11}$$

where $B_1 = 0.6961663, B_2 = 0.4079426, B_3 = 0.8974794, \lambda_1^2 = 0.004679148, \lambda_2^2 = 0.01351206$, and $\lambda_3^2 = 97.934002$. Here, $\lambda_0 = 1.273\,\mu$m. For the evaluation of 1.55-μm transmission window, we shift parallelly the dispersion curve from $\lambda_z = 1.273\,\mu$m to $\lambda_z = 1.55\,\mu$m. For the direct detection system, we take 1000 photons per bit as the detection sensitivity, so the minimum required input peak power for a Gaussian pulse can be calculated as

$$P_{\text{in}} = \frac{1000h\nu\exp(\alpha L)}{\int_{-\infty}^{\infty}\exp(-t^2/T_0^2)\,dt} \tag{12}$$

where L is the transmission distance, h is Planck's constant, and ν is the carrier frequency. The input power P_{in} will be limited to below 500 mW so that stimulated Raman scattering has no appreciable effect [13]. The Gaussian pulse is used as the input pulse with the following form for the numerical simulation:

$$u(0,\tau) = \frac{\sqrt{P_{\text{in}}}}{\sqrt{P_0}}\exp(-\tau^2/2). \tag{13}$$

Given the initial input pulse, (9) can be solved numerically by the propagation beam method [14]. We take the root-mean-square width (σ) weighted by optical intensity as a measure of the pulse width of the evolving optical pulse [1]. In the following discussion, we will take 2σ as the full pulse width.

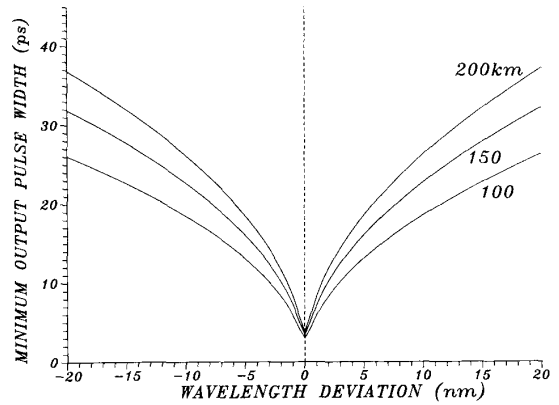

Fig. 1. Minimum output pulse width predicted by (14) versus carrier wavelength deviation for various transmission distances.

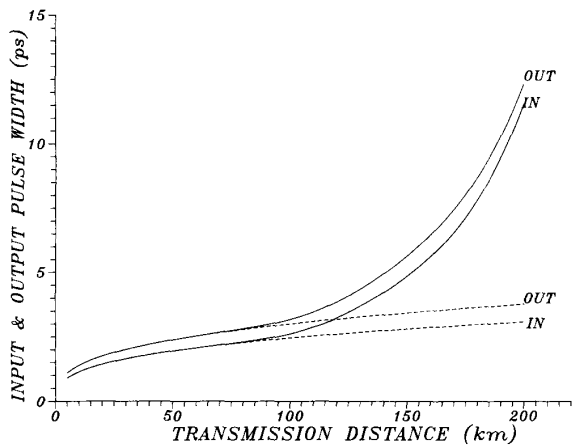

Fig. 2. Minimum output phase width and its input pulse width versus transmission distance for linear case (dashed line) and nonlinear case (solid line) when $\lambda = \lambda_0$ in both cases.

III. Results and Discussions

A. 1.55-μm Transmission Window

Without SPM effect, the Gaussian input pulses will broaden according to [11]

$$\sigma_{\text{out}} = \sigma_{\text{in}}\sqrt{1 + (\beta_2 L/T_0^2)^2 + (\beta_3 L/2T_0^3)^2} \tag{14}$$

where σ_{in} and σ_{out} are the rms widths of the input and output pulses, respectively. We know that for a given transmission distance L, there exists a minimum output pulse width for an optimum input pulse width. Fig. 1 shows the minimum output pulse width as a function of the carrier wavelength deviation, $\Delta\lambda = \lambda - \lambda_0$, for various transmission distances. Fig. 2 shows the minimum output pulse width and its input pulse width as functions of transmission distance for linear case (dashed lines) and nonlinear case (solid lines) when $\lambda = \lambda_0$ in both cases. We note that the output pulse width in nonlinear case begins to deviate away from that in linear case when $L > 80$ km. For the longer transmission distance, the higher input pulse power induces stronger SPM-effect and the output pulse

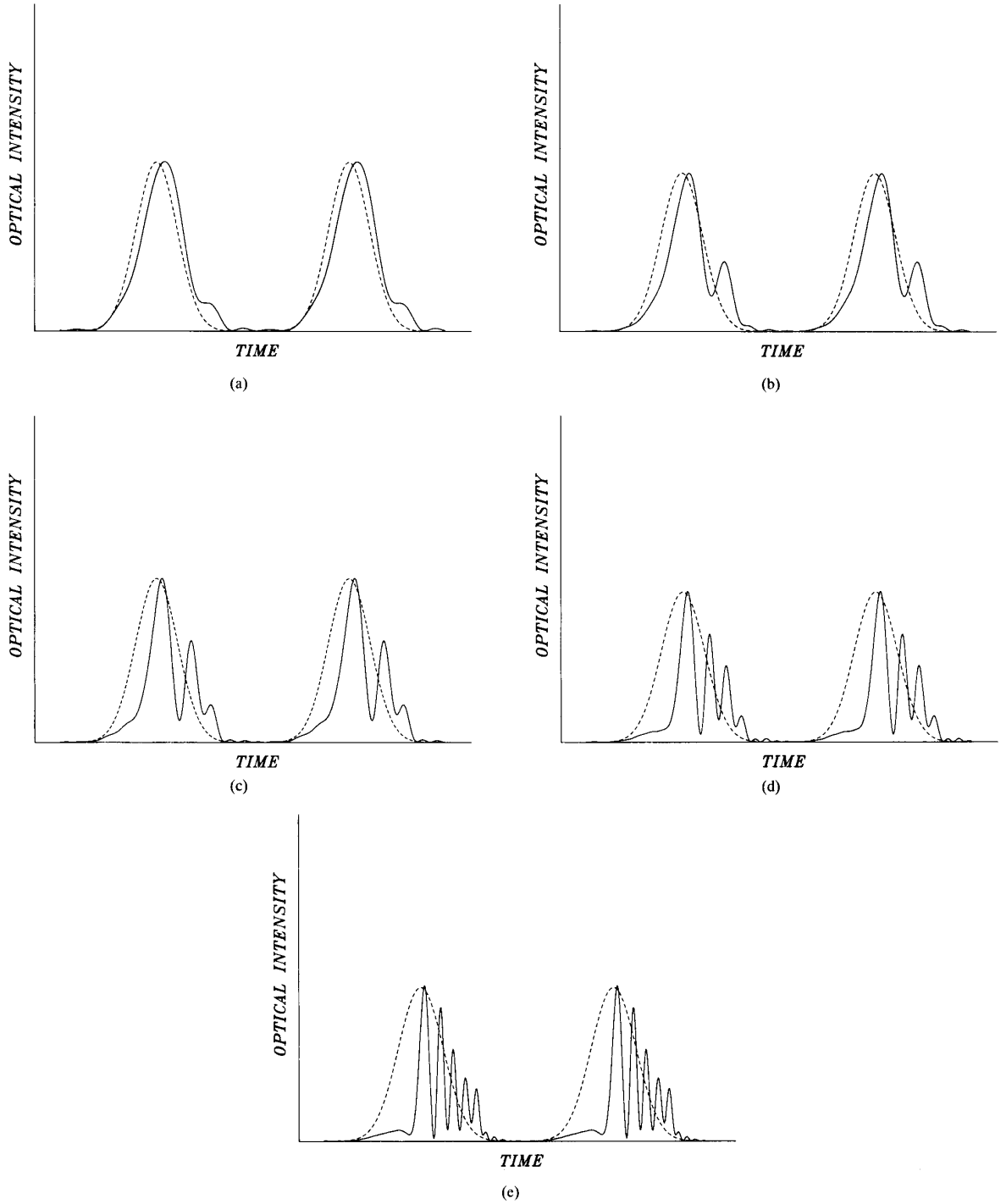

Fig. 3. The temporal profiles of initial input pulse (dashed line) and rescaled output pulse (solid line) when $\lambda = \lambda_0$. (a) $L = 130$ km, (b) $L = 150$ km, (c) $L = 165$ km, (d) $L = 180$ km, and (e) $L = 195$ km. The inter-pulse separation is four times of the output pulse width.

deteriorates more seriously. Fig. 3(a)–(e) show the input pulse (dashed line) and output pulse (solid line) when $\lambda = \lambda_0$ for $L = 130$, 150, 165, 180, and 195 km, respectively. The inter-pulse separation is chosen to be four times of the output pulse width, and the output pulses are rescaled for the convenience of comparison. A second peak begins to build up in Fig. 3(a) and grows in Fig. 3(b). The third, fourth and fifth peaks appear in Fig. 3(c), Fig. 3(d), and Fig. 3(e), respectively. Fig. 4 indicates

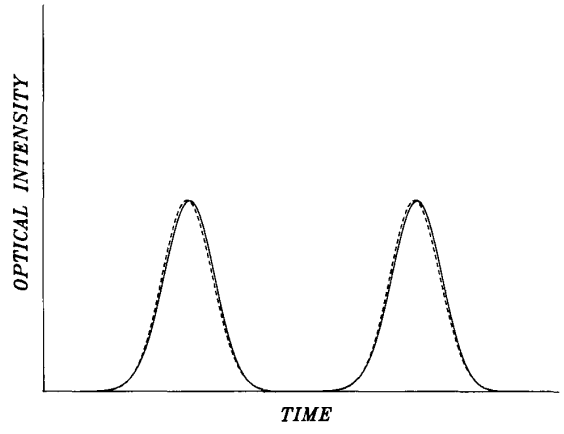

Fig. 4. The temporal profiles of initial input pulse (dashed line) and rescaled output pulse (solid line) when $\lambda = \lambda_0, L = 165$ km and the SPM effect is excluded. The inter-pulse separation is four times of the output pulse width.

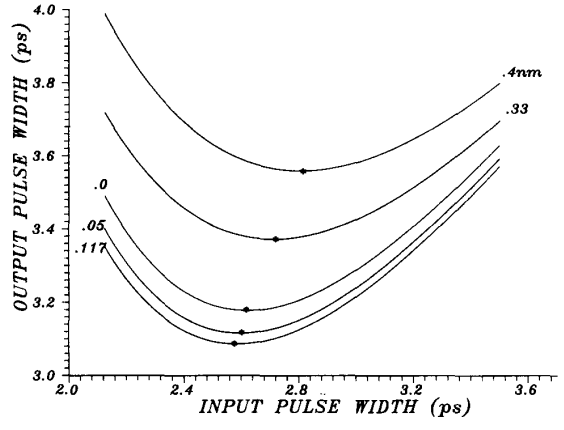

Fig. 5. Output pulse width versus input pulse width for 100-km transmission distance and various wavelength deviations.

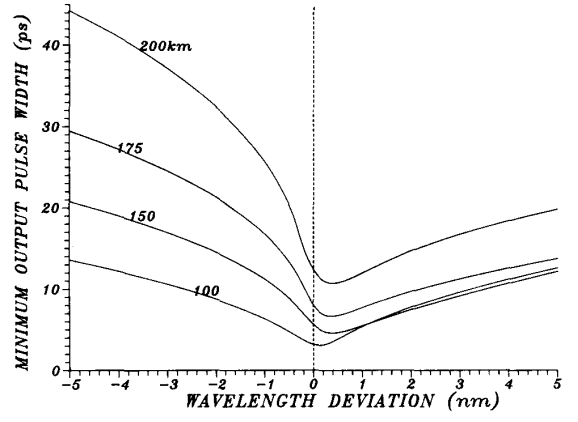

Fig. 6. Minimum output pulse width solved by (9) versus carrier wavelength deviation for various transmission distance.

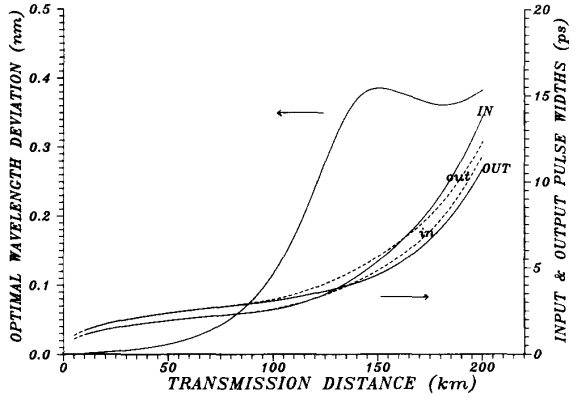

Fig. 7. Optimal carrier wavelength deviation, optimal minimum output pulse width and its input pulse width versus transmission distance (solid lines). Dashed lines indicate the minimum output pulse width and its input pulse widths when $\lambda = \lambda_0 = 1.55\mu$m.

the output pulse without SPM effect for $L = 165$ km when $\lambda = \lambda_0$. The output pulse shape (solid line) shows that the multi-peak feature results from the SPM and GVD effects instead of the second order dispersion effect.

Fig. 5 shows output pulse width against input pulse width for 100-km transmission distance and various carrier wavelength deviations. For a specific carrier wavelength deviation, there always exists a minimum output pulse width for a suitable input pulse width. The minimum output pulse width decreases with $\Delta\lambda$ until $\Delta\lambda = \Delta\lambda_{op} = 0.117$ nm. When $\Delta\lambda$ is smaller than $\Delta\lambda_{op}$ and close to zero, the SPM-broadened spectrum will span into normal dispersion region, and the dispersive tails of pulse contribute to pulse broadening so that the resulting minimum output pulse width increases as $\Delta\lambda$ decreases. This implies that for a fixed transmission length, there exists a specific carrier wavelength deviation $\Delta\lambda_{op}$ to have the optimal input and output pulse widths. Fig. 6 summarizes the minimum output pulse width versus carrier wavelength deviation for various transmission distances. In the normal dispersion region, the interaction between SPM and GVD results in excessive pulse broadening. In the anomalous dispersion region, the interaction between SPM and GVD can lead to the pulse narrowing. It is obvious that there always exists an optimum minimum output pulse width against a specific $\Delta\lambda_{op}$ for any given transmission distance. This result implies that for a fixed transmission distance, we can choose an optimal carrier wavelength deviation $\Delta\lambda_{op}$ to obtain the maximum transmission bitrate if we use the output pulse width to determine the signal bitrate.

It is also noted from Fig. 6 that the dispersion-free design is unstable for longer transmission distance, because the minimum output pulse width is very sensitive to the carrier wavelength fluctuation when $\lambda = \lambda_0$. Apparently, the system operated at the optimal carrier wavelength, $\lambda = \lambda_0 + \Delta\lambda_{op}$, is more stable than that operated at $\lambda = \lambda_0$ for longer transmission distance. Fig. 7 summarizes the optimal carrier wavelength deviation, the optimal minimum output pulse width and its input pulse width against the transmission distance where the dashed lines indicate the pulse widths in the case when $\lambda = \lambda_0$. It is observed that the increase of

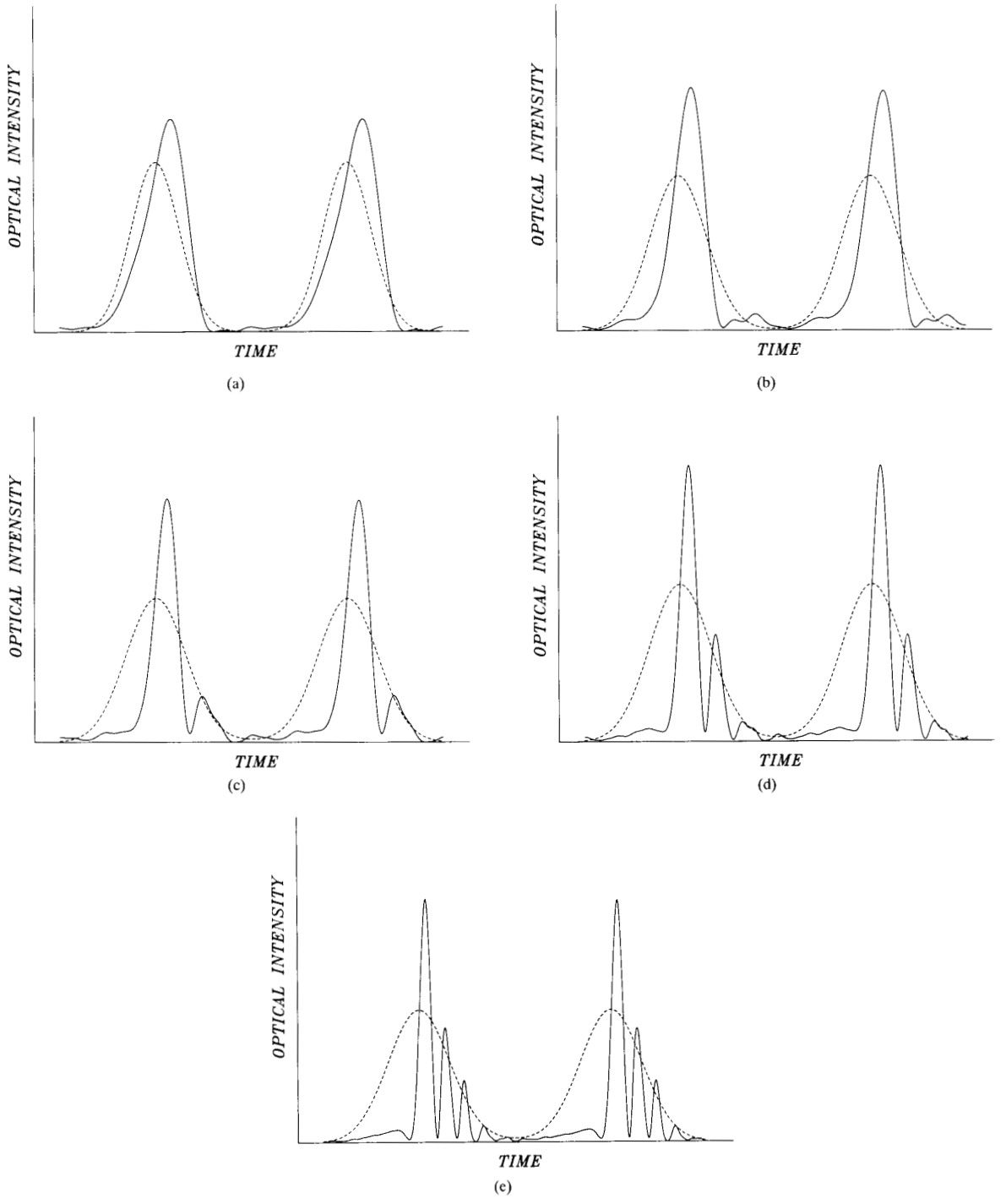

Fig. 8. The temporal profiles of initial input pulse (dashed line) and rescaled output pulse (solid line) when $\lambda = \lambda_0 + \Delta\lambda_{op}$. (a) $L = 130$ km, (b) $L = 150$ km, (c) $L = 165$ km, (d) $L = 180$ km, and (e) $L = 195$ km. The inter-pulse separation is four times of the output pulse width.

the optimal carrier wavelength deviation is gradually saturated when $L > 130$ km. For the longer transmission distance, the required input powers are larger and the SPM-induced spectrum broadenings are stronger. The optimal carrier wavelength deviation must be larger to avoid spectrum cross to the normal dispersion region. The optimal input pulse width required to achieve optimal minimum output pulse width becomes larger, i.e., the initial optical spectrum is narrower and the

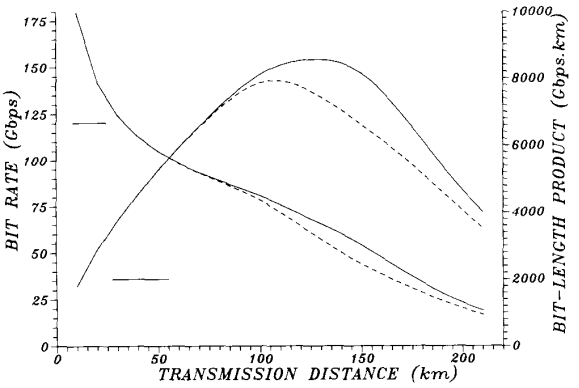

Fig. 9. The bitrate and BL product as functions of transmission distance when $\lambda = \lambda_0 + \Delta\lambda_{op}$ (solid lines) and $\lambda = \lambda_0$ (dashed lines).

smaller carrier wavelength deviation is needed. Therefore, $\Delta\lambda_{op}$ becomes saturated when the transmission distance is large enough. When $\lambda = \lambda_0$ (dashed lines), the minimum output pulse width is always larger than its input pulse width for any given transmission length. But under the optimal transmission conditions (solid lines), the output pulse widths begin to be different from the case when $\lambda = \lambda_0$ for $L > 80$ km. Fig. 8(a)–(e) are similar to Fig. 3(a)–(e) except for $\lambda = \lambda_z + \Delta\lambda_{op}$. Comparing Fig. 8(a)–(e) to Fig. 3(a)–(e) one-by-one, we note that the number of subpeaks decreases by one, the magnitudes of subpeaks reduce, and most of the pulse power is concentrated in the main peak of the output pulse. If we choose four times of output pulse width as the input pulse separation, then we can calculate and plot the optimal bitrate and bit-length (BL) product against transmission distance as shown in Fig. 9. The maximum BL product value for optimal transmission condition (solid line), $(\mathrm{BL})_{\max} = 8550$ Gb/s·km, occurs around $L = 130$ km. It is obvious that the performance of system at the optimal transmission condition has a significant improvement over the case of $\lambda = \lambda_0$ for $L > 100$ km.

B. 1.3-μm Transmission Window

With the larger fiber loss at the 1.3-μm transmission window, the required minimum input power should be stronger. Therefore, the transmission distance where the SPM-effect becomes significant decreases to about 70 km.

IV. Conclusion

Optimal transmission conditions of nonlinear optical pulses without amplification have been discussed. A bit-length product up to 8550 Gb/s · km or more has been achieved by using the Gaussian input pulses and dispersion-shifted fibers. The system performance, including the operation stability, has significant improvement over the conventional dispersion-free system design when the transmission distances are larger than 100 and 70 km for 1.55- and 1.3-μm transmission windows, respectively.

References

[1] D. Marcuse and C. Lin, "Low dispersion single-mode fiber transmission—The question of practical versus theoretical maximum transmission bandwidth," *IEEE J. Quantum Electron.*, vol. QE-17, pp. 869–878, 1981.
[2] K. J. Blow and N. J. Doran, "Nonlinear limits on bandwidth at the minimum dispersion in optical fibers," *Opt. Commun.*, vol. 48, pp. 181–184, 1983.
[3] M. Stern, J. P. Heritage, R. N. Thurston, and S. Tu, "Self-phase modulation and dispersion in high data rate fiber optic transmission systems," *J. Lightwave Technol.*, vol. 8, pp. 1009–1016, 1990.
[4] A. Hasegawa and F. Tappert, "Transmission of stationary nonlinear optical pulses in dispersive dielectric fibers, I. Anomalous dispersion," *Appl. Phys. Lett.*, vol. 23, pp. 142–144, 173.
[5] A. Hasegawa and Y. Kodama, "Signal transmission by optical solitons in monomode fiber," *Proc. IEEE*, vol. 69, pp. 1145–1150, 1981.
[6] K. J. Blow and N. J. Doran, "High bit rate communication systems using nonlinear effects," *Opt. Commun.*, vol. 42, pp. 403–406, 1982.
[7] M. J. Potasek and G. P. Agrawal, "Power-dependent enhancement in repeater spacing for dispersion-limited optical communication system," *Electron. Lett.*, vol. 22, pp. 759–760, 1986.
[8] G. Veith, "Useful and detrimental aspects of self-phase modulation in fiber optical amplifiers," *SPIE Proc. Advanced Opto-Electron. Technol.*, vol. 64, pp. 205–214, 1988.
[9] G. R. Boyer and X. F. Carlotti, "Nonlinear propagation in a single-mode optical fiber in case of small group velocity dispersion," *Opt. Commun.*, vol. 15, pp. 18–22, 1986.
[10] G. P. Agrawal and M. J. Potasek, "Nonlinear pulse distortion in single-mode optical fibers at the zero-dispersion wavelength," *Phys. Rev. A*, vol. 22, pp. 1765–1776, 1986.
[11] G. P. Agrawal, *Nonlinear Fiber Optics.* Boston: Academic, 1989.
[12] D. Marcuse, "Pulse distortion in single-mode fiber," *Appl. Opt.*, vol. 19, pp. 1653–1660, 1980.
[13] R. H. Stolen, J. P. Gordon, W. J. Tomlinson, and H. A. Haus, "Raman response function of silica-core fibers," *J. Opt. Soc. Amer. B*, vol. 6, pp. 1159–1166, 1988.
[14] D. Yevick and B. Hermansson, "Soliton analysis with the propagation beam method," *Opt. Commun.*, vol. 47, pp. 101–106, 1983.

Min-Chuan Lin was born on December 25, 1956, in Jiangwha, Taiwan, Republic of China. He received the B.S.E.E. degree from National University in 1979, the M.S. and Ph.D. degrees in electro-optical engineering from National Chiao Tung University, Taiwan, in 1987 and 1922, respectively.

He is now an Associate Professor in the Electrical Engineering Department at Kuan San Institute of Technology, Tainan, Taiwan, Republic of China.

Sien Chi was born on July 6, 1936, in Huaiying, Jiangsu, China. He received the B.S.E.E. degree from National Taiwan University and the M.S.E.E. degree from National Chiao Tung Universtiy, Taiwan, R.O.C., in 1959 and 1961, respectively. He received the Ph.D. degree in electrophysics from the Polytechnic Institute of Brooklyn, Brooklyn, NY, in 1971.

In 1971, he joined the faculty of National Chiao Tung University, where he is currently a Professor of Electro-optical Engineering. From 1977 to 1978 he was a resident visitor at Bell Laboratories, Holmdel, NJ. From 1986 to 1987 he took a sabbatical leave to Hua Eng Wires and Cables, Taiwan, where he conducted research programs in fiber optics. His research interests are in the area of fiber and nonlinear optics.